Zeitschrift: IABSE congress report = Rapport du congrès AIPC = IVBH Kongressbericht

Band: 9 (1972)

Artikel: Post-critical behaviour of inelastic structures

Autor: Augusti, Giuliano

DOI: https://doi.org/10.5169/seals-9546

Nutzungsbedingungen

Die ETH-Bibliothek ist die Anbieterin der digitalisierten Zeitschriften. Sie besitzt keine Urheberrechte an den Zeitschriften und ist nicht verantwortlich für deren Inhalte. Die Rechte liegen in der Regel bei den Herausgebern beziehungsweise den externen Rechteinhabern. Siehe Rechtliche Hinweise.

Conditions d'utilisation

L'ETH Library est le fournisseur des revues numérisées. Elle ne détient aucun droit d'auteur sur les revues et n'est pas responsable de leur contenu. En règle générale, les droits sont détenus par les éditeurs ou les détenteurs de droits externes. Voir Informations légales.

Terms of use

The ETH Library is the provider of the digitised journals. It does not own any copyrights to the journals and is not responsible for their content. The rights usually lie with the publishers or the external rights holders. See Legal notice.

Download PDF: 15.03.2025

ETH-Bibliothek Zürich, E-Periodica, https://www.e-periodica.ch

Post-Critical Behaviour of Inelastic Structures

Comportement post-critique de structures non-élastiques

Überkritisches Verhalten unelastischer Träger

GIULIANO AUGUSTI
Assoc. Professor of Structural Engineering
Università di Firenze
Florence, Italy

As illustrated by Professor Bieniek's Report, it is now increasingly recognized that in structural engineering the knowledge of the post-critical behaviour is almost as essential as that of the critical load itself: in fact, the unavoidable imperfections that make actual structures different from the "ideally perfect" models of applied mechanics, affect their strength in a way that depends largely on the post-critical behaviour of their "ideally perfect" models.

This contribution presents an elementary (but hopefully stimulating) discussion of the joint effects of imperfections and inelastic deformations on the behaviour of structures that, if perfect, would exhibit a point of bifurcation of equilibrium. As in Ref. (A.1) (°), buckling will be used as a synonym for bifurcation of equilibrium, while collapse load will indicate a (local) maximum on an actual load-deformation path. Dynamical and time-rate effects will not be considered.

The most rational approach to the study of the effect of imperfections on structural strength is through statistics and probability theory, as indicated by Bieniek (p.38) and proved by an increasing number of research papers. From this point of view, an actual structure is seen as a sample structure taken out of a population of nominally identical structures, different from each other because of random variations of the design parameters (yield stress, geometric dimensions, etc.). The ideal structure, corresponding exactly to the design, is the average structure of this population. With some qualifications (°°), it can be stated that the average (expected) strength of the actual structure is approximately equal to the strength of the average structure in absence of phenomena of geometrical instability, and is lower if these phenomena are present. In the latter case, the introduction of probabilistic methods becomes of utmost importance in order to obtain economical and reliable designs. This point is illustrated, in the following Section 1, by the summary of a probabilistic investigation

---

(°) See list of References at the end of this contribution.

(°°) The following statement is too general to be more than an approximation. For instance, it has already been proved (A.2) that the average plastic collapse load of a ductile structure is smaller than the collapse load of the average structure, but in the first numerical examples their difference is rather small.

of slender imperfect columns, fully published elsewhere (A.3). A basic difference between this study and previous works by other Authors is the introduction of other random quantities (namely, the yield stress and the free buckling length) besides the geometrical imperfections.

In Ref. (A.3), collapse occurs because inelastic deformations develop: this appears to be the most frequent cause of collapse of actual structures, and it is rather surprising that the interaction of inelasticity and instability is still a comparatively little-explored field, perhaps avoided by most researchers because of its great analytical difficulties.

Section 2 below presents two examples of asymmetric behaviour (i.e., of load-deformation paths that depend on the sign of the deformation) of structures that, if perfect, would buckle elastically. In the first example, the asymmetry occurs in the inelastic range of deformations and is due to an asymmetry in the strength of structural cross-section. The second example illustrates asymmetric elastic buckling, a phenomenon now well known, after the great amount of research spurred by Koiter's fundamental works (Bieniek's Refs. 47 and 71), and apparently the only practically significant case in which collapse may be completely independent of the onset of inelastic deformations.

Finally, the last Section of this paper discusses and compares different cases of buckling in the inelastic range. Again, it will be shown that either a strength asymmetry or a geometry effect may cause asymmetry of the post-buckling load-deformation paths of the "perfect" structure: consequently, in such cases the collapse load of the actual structure depends on the sign of the imperfection.

1) ELASTIC BUCKLING AND PLASTIC COLLAPSE: A PROBABILISTIC ANALYSIS

Consider a simple compressed strut, for instance pin-ended as in Fig. 1.1, and made of an elastic-perfectly plastic material with yield stress σ_y. If the strut is initially perfectly straight, it is well known that it remains

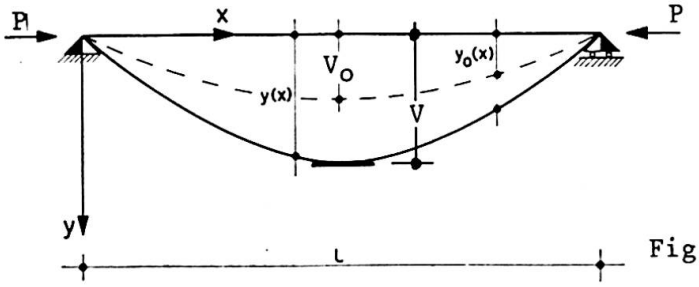

Fig. 1.1

straight and stable as long as the compressive load P is smaller than both the elastic buckling load

$$P_E = \pi^2 EI/l^2 = \pi^2 EA/\lambda^2 = \sigma_E A \quad \text{and the squash load} \quad P_y = \sigma_y A$$

If $P_E < P_y$, the load remains constant at $P = P_E$ (within the first-order, small-displacements theory) in the early stages of buckling, and begins decreasing as soon as the first plastic deformations take place; the axial load vs. mid-span displacement (P-V) path remains below, and tends asymptotically to, the P-V curve corresponding to full yielding of the cross-section $V = M_p/P$ (Fig. 1.2a): both curves have a horizontal asymptote at P = 0.

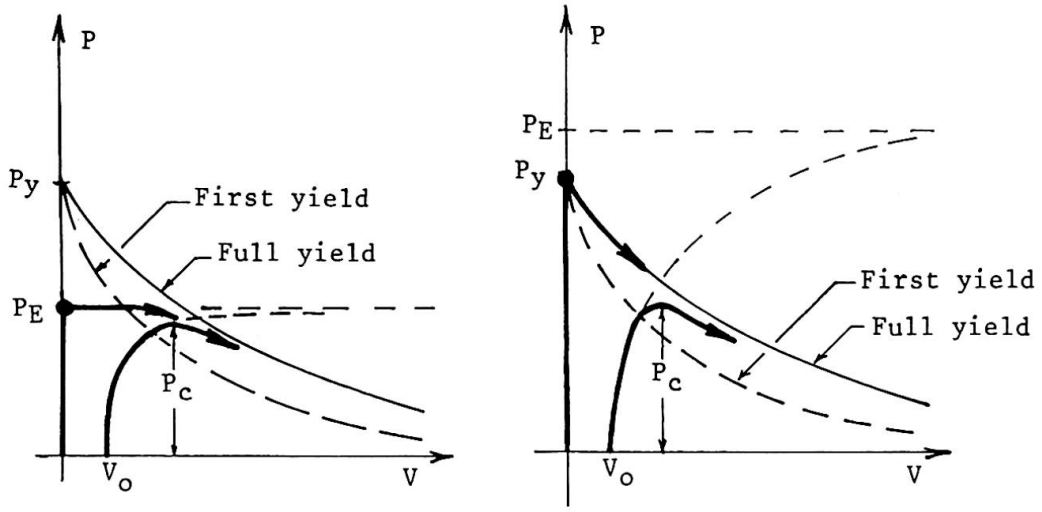

Fig. 1.2

If $P_y \leq P_E$, the strut buckles at $P = P_y$; the load P starts decreasing quite rapidly at the very onset of the deformations following the full-yield curve, and again tends asymptotically to zero when $V \to \infty$ (Fig. 1.2b).

If the material has a constant, non-zero tangent modulus E_T in the inelastic range, the horizontal asymptotes are at the load $P = P_K$ (defined in Section 3) rather than at $P = 0$ (A.4).

If the strut is affected by an initial geometrical imperfection, for instance in the form of a half sine-wave

$$Y_o = Y_o(x) = V_o \sin \pi x/l \tag{1.1}$$

(Fig. 1.1), the P-V path in the elastic range is given, with very good approximation, by (Fig. 1.2)

$$V = V_o / (1-P/P_E) \tag{1.2}$$

The actual elastic-plastic path remains below the full-yield curve: collapse occurs when sufficient plastic deformations have developed. The relation between imperfection magnitude and collapse load P_c of the type (A.3)

$$\gamma = \frac{V_o}{r} = 3 \left[\frac{P_y}{P_c} - 1\right] \left[1 - \sqrt[3]{\frac{P_c}{P_E}}\right] \tag{1.3}$$

where r is the relevant core radius of the section.

If the relationship between P_c and γ is known and γ is a random variable, it is conceptually easy to obtain the probability distribution of the dependent random variable P_c or $\sigma_c = P_c/A$. In Ref.(A.3), eq.(1.3) was assumed to hold throughout the relevant range; and, since the geometrical imperfection is essentially due to errors of fabrication with respect to the straight strut one aims at, it appeared logical to take γ to be normally distributed with zero mean, although only its absolute value, γ , appears in eq.(1.3). Fig.1.3 shows typical probability density curves of the collapse stress σ_c, calculated under the

lg. 6 Vorbericht

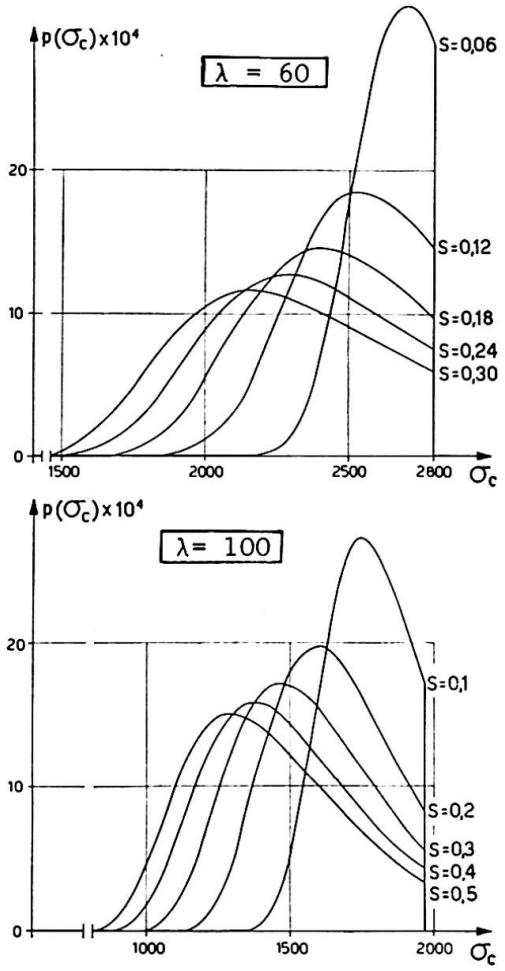

Fig. 1.3

above assumptions for the yield stress σ_y = 2800 kg/cm^2, two slenderness ratios λ, and several values of the standard variation, s, of the imperfection coefficient γ. All these curves show a sharp cut-off at the collapse stress of the imperfect strut

$$\sigma_{co} = P_{co}/A = \min(\sigma_y, \sigma_E): \quad \sigma_{co} = \sigma_y$$

when $\lambda = 60$, $\sigma_{co} = \sigma_E = P_E/A$ when $\lambda = 100$.

For a more realistic treatment, one must remember that the yield stress of a given material is also a random quantity : some earlier investigations seem to suggest that, at least in a first approximation, it can be considered to be normally distributed with a standard deviation, t, equal to about 10% of its mean value $\bar{\sigma}_y$. In the already quoted Ref. (A.3), it seemed appropriate to introduce also a random variability of the slenderness ratio λ, because this quantity may be different from the design value because of defective restraints and/or approximations introduced in the calculations; also λ has been assumed to be normally distributed, and its standard deviation, k, has been taken equal to 10% of the average value $\bar{\lambda}$. With these assumptions, the probability density curves of the collapse stress σ_c take the form shown in Fig. 1.4 : the upper cut-off disappears,

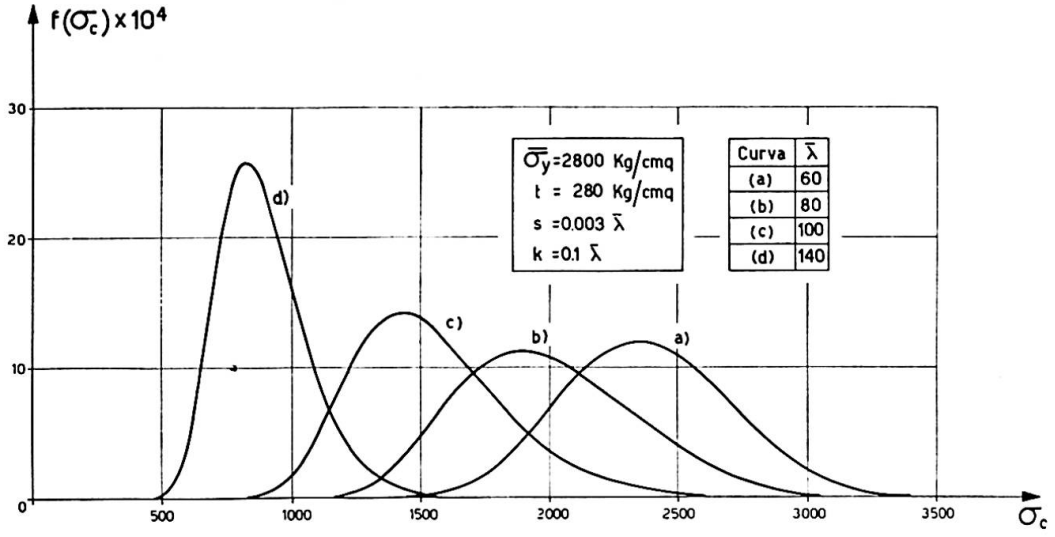

Fig. 1.4

because large values of σ_{co} are now possible, albeit with little probability. However, the average collapse stress $\bar{\sigma}_c$ remains much smaller than the collapse stress of the average, straight strut, $\sigma_{co} = \min(\bar{\sigma}_y, \bar{\sigma}_E)$.

In order to have indications for actual design practice, the relationship has also been investigated between the nominal safety factor ψ introduced in the calculations (ratio of nominal collapse stress σ_{co} to design admissible stress σ_{cam}) and the probability of collapse

$$P^* = \text{Prob}\ (\sigma_c \leq \sigma_{cam}) \tag{1.4}$$

A typical set of curves, plotted in semi-logarithmic scale in the relevant range of (very small) values of P^*, is shown in Fig. 1.5 : they can be well approximated by a set of parallel straight lines. It is also worth noting that very small variations of the nominal safety factor ψ can easily induce ten- or hundred-fold variations of actual safety; this clearly calls for a "rationalization" of design practice through the probabilistic approach. A qualitative and quantitative comparison between the results of the probabilistic treatment just summarized and the Italian Steel Building Code has also been presented in Ref. (A.3).

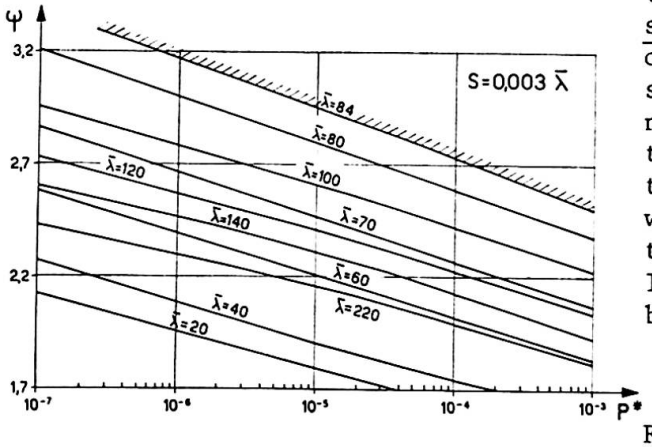

Fig. 1.5

2) ELASTIC BUCKLING: ASYMMETRIC BEHAVIOUR

The behaviour described in Section 1 is, within the elastic range, perfectly symmetrical with respect to the sign of the displacement and/or the imperfection, regardless of a possible asymmetry of the strut cross-section with respect to the axis of bending : in fact, the geometry of the section affects the behaviour of strut only through its moment of inertia. This type of behaviour (symmetric elastic buckling) is not limited exclusively to the pin-ended strut, but is common to many of the elastic structures that are liable to instability : indeed, before the development of Koiter's theory (Bieniek's Refs. 47 and 71), it was thought to be common to them all.

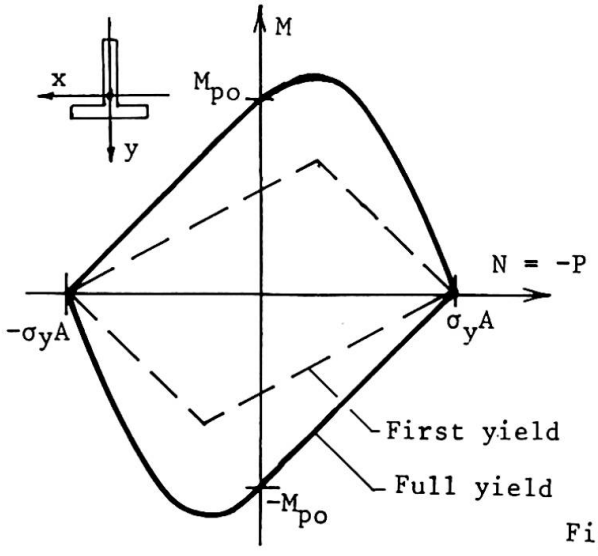

Fig. 2.1

However, the symmetry of behaviour does not extend beyond the elastic range of deformation, unless the strength of the cross-section is symmetric (as it has implicitly been assumed throughout Section 1). For instance, if the strut of Fig. 1.1 has a T-section, the first- and full-yield interaction curves in the moment-axial load (M-N) plane are qualitatively indicated in Fig. 2.1. (For a detailed derivation, cf. Ref. (A.5).)

Transformed into P–v coordinates, the interaction curves appear like in Fig. 2.2, and the P–v equilibrium paths become, on the whole, asymmetric for both

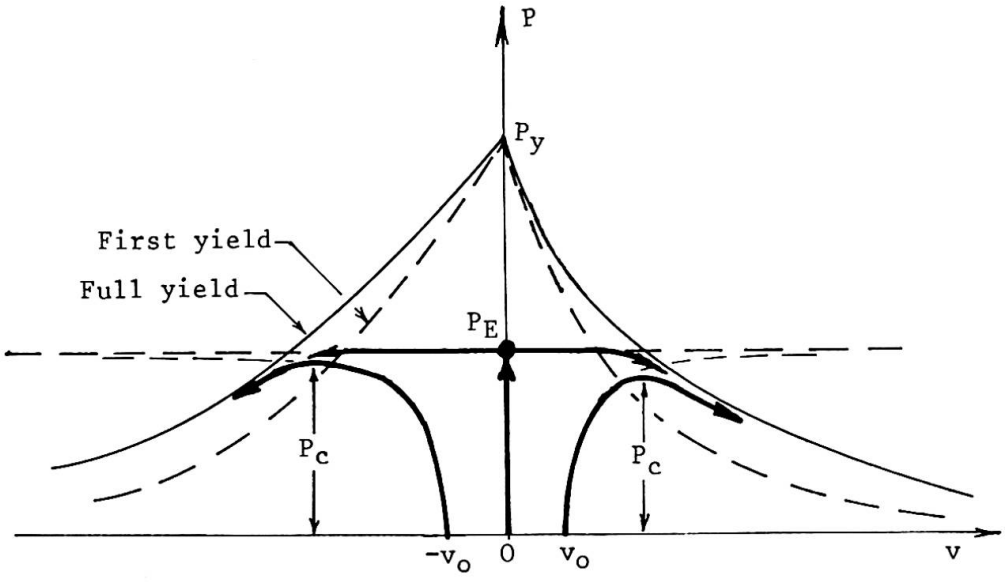

Fig. 2.2

the perfect and the imperfect strut, in both cases $P_E < P_y$ (illustrated by Fig. 2.2) and $P_y \leq P_E$ In particular, the collapse load does depend on the sign of the imperfection

$$P_c\,(V_o) \neq P_c\,(-V_o) \qquad (2.1)$$

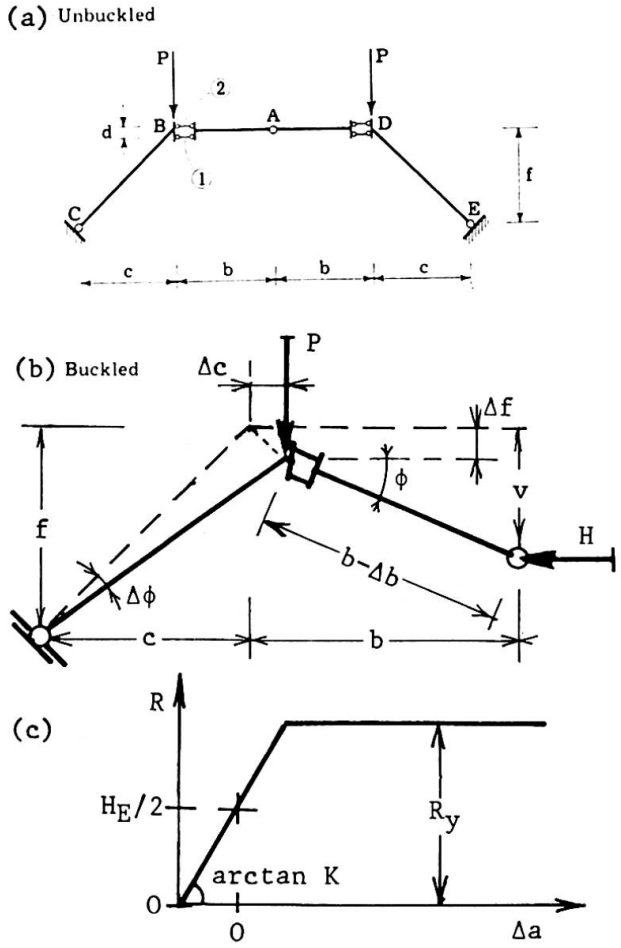

Fig. 2.3

The preceding discussion has illustrated the case of symmetric elastic buckling, followed by asymmetric plastic collapse due to an asymmetry of the cross-section : an asymmetry of yield stress (different yield points in tension and compression) would have the same qualitative effect.

Another important case of asymmetric behaviour is that of asymmetric elastic buckling, analytically described in the already quoted works by Koiter and here illustrated by the simple model of a three-hinged arch shown in Fig. 2.3a: AB, BC, etc. are rigid links; A, C, E are momentless hinges; the two deformable cells B and D consist of two parallel elastic rods (1 and 2) and a soft core that does not allow a shear deformation of the cell. Assume that Fig.2.3a represents the configuration at the point of buckling with a load $P = P_E$ and a horizontal thrust

$$H_E = P_E\, c/f \qquad (2.2)$$

The following treatment is limited to geometrically symmetrical buckled configurations, such as in Fig. 2.3b; equilibrium yields

$$\begin{aligned} P\ (c + \Delta c) &= H\ (f - v) \\ H\ (v - \Delta f) &= (R_1 - R_2)\ \frac{d}{2} \\ H &= R_1 + R_2 \end{aligned} \qquad (2.3)$$

where R_1 and R_2 are the (compressive) reactions in the elastic rods, related to their variation of length by (Fig. 2.3c)

$$K\ \Delta a_i = R_i - H_E/2 \qquad (i = 1,2) \qquad (2.4)$$

Δa_i is measured with respect to the point of buckling, and is taken positive when a shortening.

In deriving the post-buckling P-v relationship, introduce firstly the (wrong) assumption that the deformable cells do not change length during the deformation. Then geometry yields, up to second-order infinitesimals

$$(\phi - \Delta\phi)\ d = \Delta a_1 - \Delta a_2 \qquad (2.5)$$

$$\Delta c = b\ (1 - \cos\phi) = \frac{b\ \phi^2}{2} \quad ; \quad \Delta f = \frac{c}{f}\ \Delta c = \frac{bc}{f}\ \frac{\phi^2}{2} \qquad (2.6)$$

$$\phi = \frac{v - \Delta f}{b} = \frac{v}{b} - \frac{c}{f}\ \frac{\phi^2}{2} \quad ; \quad \Delta\phi = \frac{\Delta f}{c} = \frac{\Delta c}{f} = \frac{b}{f}\ \frac{\phi^2}{2} \qquad (2.7)$$

Introducing into eqs. (2.3), taking account of (2.4) and letting

$$P_E = H_E\ \frac{f}{c} = K\ \frac{d^2}{2b}\ \frac{f}{c} \qquad (2.8)$$

some algebra leads to the following expression

$$P = P_E\ (1 - \frac{3}{2}\ \frac{v}{f} + \ldots) \qquad (2.9)$$

Note that neglecting the second-order quantities $\Delta\phi$, Δc and Δf in the initial equations (2.3), the final equation would be

$$P = P_E\ (1 - \frac{v}{f}) \qquad (2.10)$$

i.e. would present an error of the same order of v : the possibility of such an error was pointed out by Koiter with reference to a simple fully elastic frame (A.6).

Actually, during buckling, the length of the elastic cells decreases of the quantity

$$\Delta b = (\Delta a_1 + \Delta a_2)\ /\ 2 \qquad (2.11)$$

Eqs. (2.6a) and (2.7b) become respectively

$$\Delta c = (b - \Delta b)\ (1 - \cos\phi) = b(\frac{\phi^2}{2} + \frac{\Delta b}{b}) \qquad (2.12)$$

$$\Delta\phi = \frac{\Delta c}{f} = \frac{b}{f}\ (\frac{\phi^2}{2} + \frac{\Delta b}{b})$$

Introducing these new expressions into (2.3) and (2.4) and rearranging, one obtains

$$2\,\phi\,\frac{\Delta b}{b} = -\frac{d^2}{2f}\left(\frac{\phi^2}{2} + \frac{\Delta b}{b}\right) \tag{2.13}$$

so that, up to second-order terms,

$$\frac{\Delta b}{b} = -\frac{\phi^2}{2} \quad ; \quad \Delta c = \Delta f = \Delta\phi = 0 \tag{2.14}$$

and eq. (2.10) holds, at least in the vicinity of the P-axis: this equation has been accepted in an earlier presentation of this arch model (A.7).

The limit condition of the arch corresponds to the most stressed rod reaching its yield value R_y (Fig.2.3c): the first- and full-yield M-N interaction profiles of the cells coincide into a diamond (Fig.2.4). Neglecting, in accord with eq. (2.14), all second-order displacements, it is easy to transform this diamond into the following P-v curves:

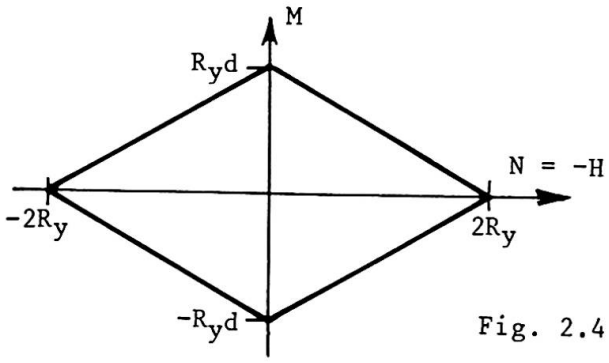

Fig. 2.4

$$v > 0;\ R_1 = R_y;\ P = P_y\,\frac{1-v/f}{1+2\,v/d} \tag{2.15}$$

$$v < 0;\ R_2 = R_y;\ P = P_y\,\frac{1-v/f}{1-2\,v/d} \tag{2.16}$$

where

$$P_y = 2\,R_y\,f/c \tag{2.17}$$

Eqs. (2.15) and (2.16), qualitatively sketched in Fig. 2.5, have the horizontal asymptote

$$P = \mp\,P_y\,d/2f \tag{2.18}$$

respectively; eq. (2.15) intersects the v-axis at v = f, with a slope

$$\left[\frac{dP}{dv}\right]_{P=0} = -\frac{P_y}{f}\,\frac{1}{1+2\,f/d} \tag{2.19}$$

so that, provided $P_y > P_E > P_y/(1+2\,f/d)$, eq.(2.10) intersects both eqs. (2.15) and (2.16) (Fig. 2.5). In words, elastic buckling of the perfect elastic arch just described is followed by compression yielding in the deformable cell.

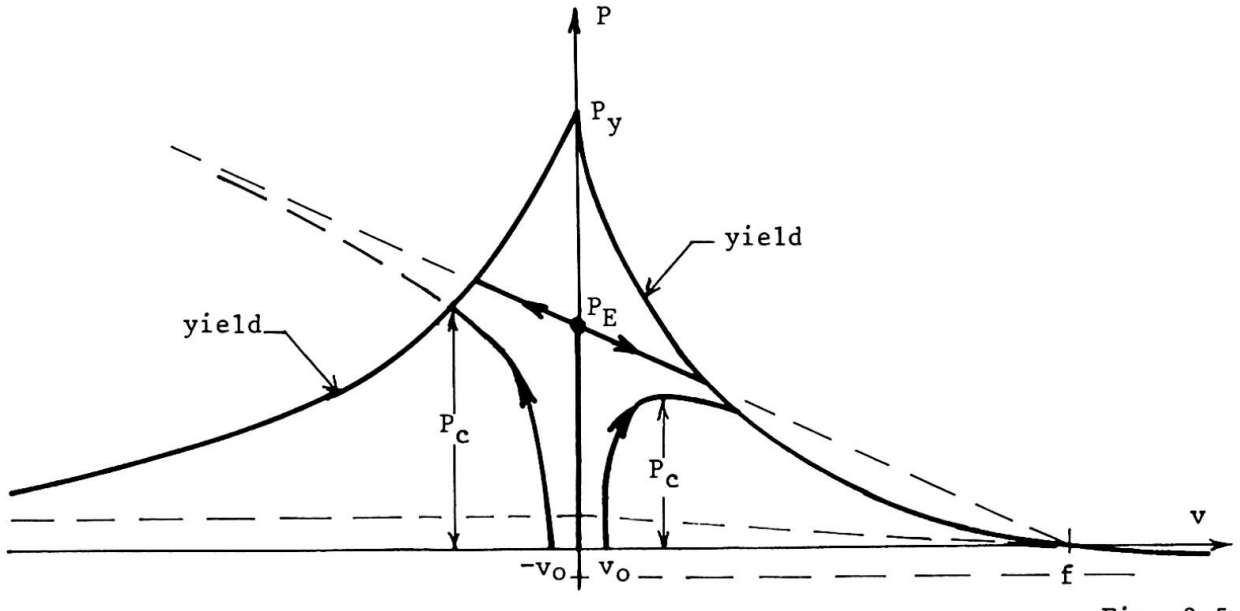

Fig. 2.5

If an initial imperfection, v_o, is present, the elastic P-v paths tend asymptotically to the straight line, eq. (2.10). Therefore, as shown in Fig. 2.5, when $v_o > 0$ the collapse load P_c is most probably reached within the elastic range of behaviour, while if $v_o < 0$ collapse occurs at the yield limit curve. It is thus shown that, in a structure liable to asymmetric elastic buckling, (a) the sign of the imperfection may affect the value of the collapse load as well as the qualitative type of collapse; and (b) the possibility of yielding may have no influence on collapse, if the imperfection weakens the structure.

3) STRUCTURES THAT BUCKLE IN THE INELASTIC RANGE

If the structural material is elastic-perfectly plastic, inelastic buckling occurs, under a rapidly decreasing load, when $P_y < P_E$, as in Fig.1.2b: the corresponding modifications of Figs. 2.2 and 2.5 are immediate. If the material has a non-zero inelastic modulus E_T, the simplest case of buckling beyond the elastic range is well illustrated by the well known Shanley's strut model (A.8). Assuming a constant modulus E_T and elastic unloading (Fig. 3.1),

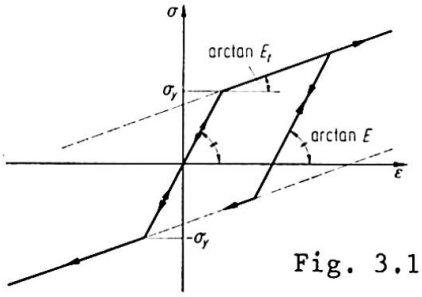

Fig. 3.1

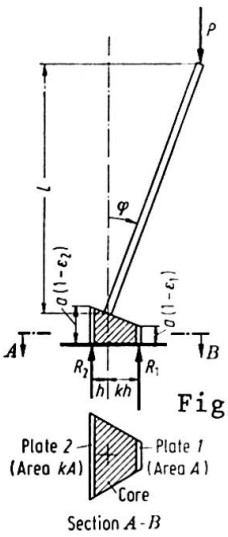

Fig. 3.3

Fig. 3.2

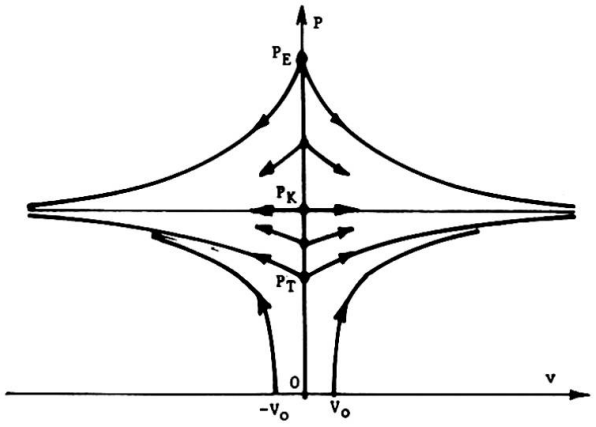

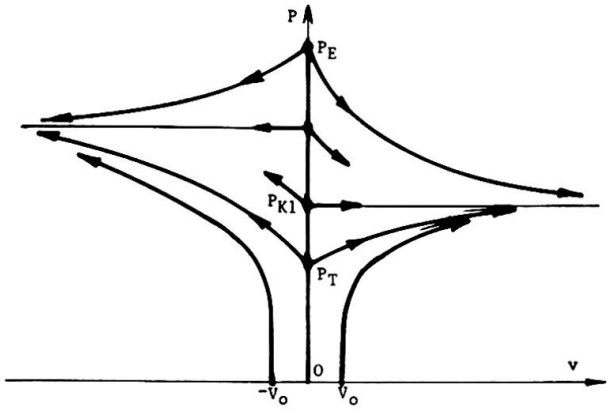

Fig. 3.4

the inelastic perfect strut may buckle at any load comprised between P_T and P_E; all P-v paths have a horizontal asymptote at a load $P = P_K \in (P_T, P_E)$, so that the load increases with $|v|$ (and the strut is stable,(A.1)) if buckling starts between P_T and P_K, decreases if buckling starts between P_K and P_E(°). The

(°) The validity of these statements is limited to comparatively small values of v. Otherwise, not only the small-displacements approximation loses validity, but the material may yield in tension in the "unloading" zone, or E_T may vary in the "loading" zone. Note that the latter probably occurs before the former in a real material, at least in the more significant range $P \leq P_K$, where the average stress $\sigma = P/A$ increases with the deformation.

loads P_T and P_K are obtained from the formula for the elastic buckling load P_E, substituting the elastic (Young's) modulus E, respectively with the tangent modulus E_T and with the so-called reduced modulus E_K, that depends on E, E_T and the shape of the section.

If the strut is not initially straight, the P-v path lies on either side of the P-axis according to the sign of the initial imperfection v_o, and below the lowest path of the perfect strut (which starts from $P = P_T$, Fig.3.2), to which path it tends when $v_o \to 0$. But some degree of imperfection is unavoidable in an actual structure; therefore, of the infinite theoretically possible buckling paths, only the lowest ones seem to be significant from an engineering point of view. Collapse of the inelastic strut, be it perfect or not, occurs with one of the phenomena mentioned in the footnote on the previous page; for detailed examples see e.g. Refs.(A.4) and (A.9) dealing respectively with Shanley's model and with the practically important case of mild steel columns with residual stresses.

In Shanley's treatment and in the above description, the strut cross-section is assumed to be symmetric with respect to the axis of bending: the whole picture in Fig.3.2 is also symmetric with respect to the P-axis. But if the cross-section is not symmetric (as in the example of Fig.3.3, Ref.(A.1)) the buckling interval of the perfect strut (P_T, P_E) remains unique, but each P-v path is different for $v > 0$ and $v < 0$, including the initial slope $[dP/dv]_{v=0}$ and the horizontal asymptote (Fig.3.4). In case of inelastic buckling, therefore, an asymmetry of strength implies asymmetric behaviour from the first stages of deformation. Again, the P-v path of any imperfect strut "is below the relevant lowest branch of the perfect strut ... and tends to such branch when the imperfection tends to zero" (A.1); the effects of an imperfection clearly depend on its sign.

The previous examples illustrate the inelastic behaviour of structures that, in the elastic range, exhibit symmetric buckling. The model arch of Fig.(2.3) was used in Ref.(A.7) to exemplify the inelastic behaviour of a structure liable to asymmetric elastic buckling; the effects of imperfections on this model have been investigated in detail by Batterman (A.10). Another simple model and a more realistic example have been presented by Hutchinson (A.11), with qualitatively similar results.

Referring to (A.9) and (A.10) for the analytical treatment (°), the behaviour of the perfect arch is summarized by Fig.3.5, and that of the imperfect arch by Fig.3.6 (reproduced from (A.10)).

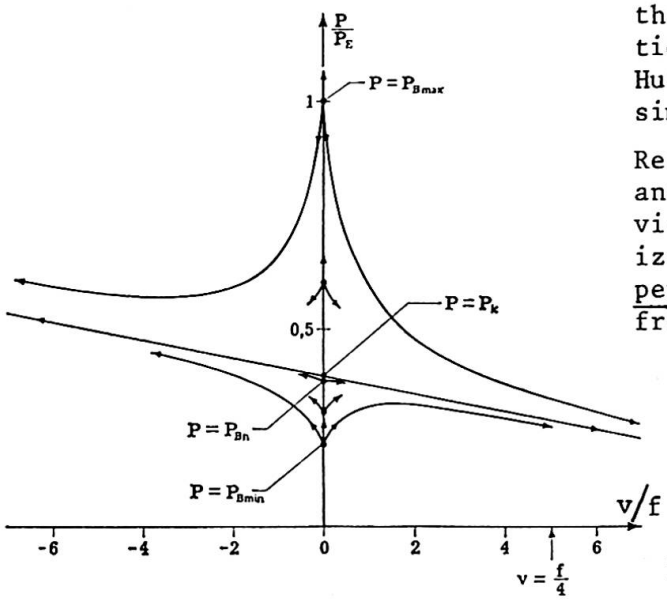

Fig. 3.5

(°) The second-order quantities Δc, Δf, etc., were neglected in the analysis (cf. eqs.(2.3) seqq.). This can be approximately justified, for small v, by the result of the complete elastic analysis, eqs.(2.14) and (2.10).

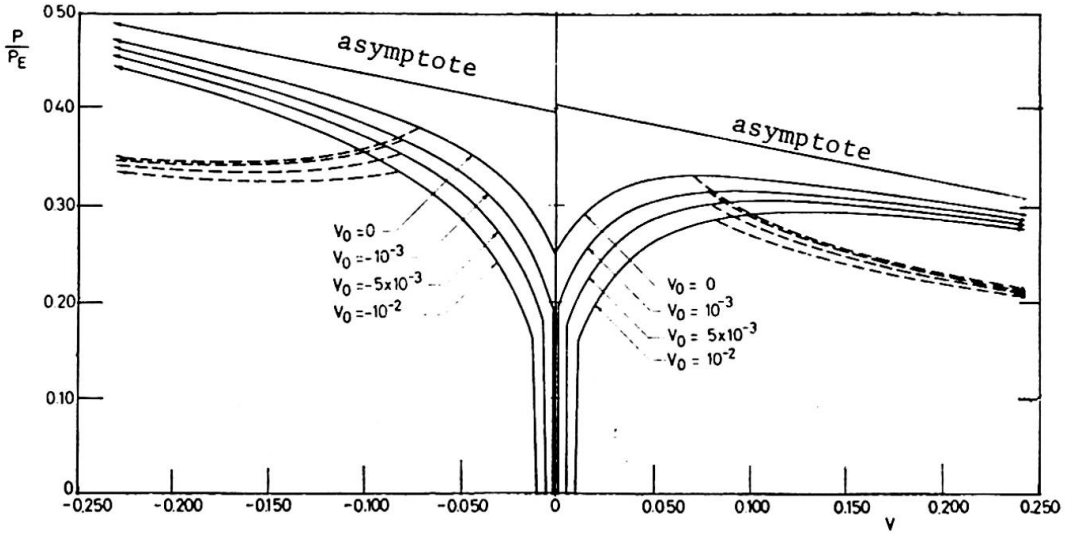

Fig. 3.6

Inspection of these Figures shows that the behaviour of the arch is markedly asymmetric, in the sense that it depends strongly on the sign of the displacement (and the initial imperfection). As in the previous examples, all paths of the imperfect structure ($v_o \neq 0$) lie below the lowest paths of the perfect one ($v_o = 0$) and tend to either of these when $v_o \to 0$ (Fig. 3.6); the straight asymptotes have a finite slope and, as noted by Batterman, are different on either side of the P-axis. The perfect arch is stable, for zero displacement, up to a load indicated by P_{Bn} in Fig. 3.5; but, when buckling with positive v, it always reaches a collapse point and becomes unstable. The imperfect arch collapses only (and always) when $v_o > 0$, unless account is taken of the possibility of tension yielding (which leads to the dashed lines of Fig.3.6) or of a decrease in E_T.

The behaviour illustrated by Figs. 3.5 and 3.6 is the inelastic analogue of Koiter's asymmetric elastic buckling.

REFERENCES

(A.1) G. Augusti, Instability of Continuous Systems (IUTAM Symposium Herrenalb 1969, edited by H. Leipholz), pp.175-182; Springer, Berlin 1971.
(A.2) G. Augusti and A. Baratta, Journ.Structural Mechanics, 1, No.1, 1972.
(A.3) G. Augusti and A. Baratta, Costruzioni Metalliche, 23, No.1, 1971 (in Italian) and Construction Metallique, 8, No.2, 1971 (in French).
(A.4) G. Augusti, Ingegneria Civile, No.11, 1964.
(A.5) J. Baker and J. Heyman, Plastic Design of Frames, Vol.I, pp.25-28; Cambridge Univ. Press 1969.
(A.6) W.T. Koiter, Recent Progress in Applied Mechanics (The Folke Odqvist Volume); pp.337-354; Almqvist & Wiksell, Stockholm 1967.
(A.7) G. Augusti, Meccanica (AIMETA), 3, No.2, 1968.
(A.8) F.R. Shanley, J.Aero.Sci., 14, No.5, 1947.
(A.9) G. Augusti, Journ.Engrg.Mech.Div., ASCE, 91, No.EM4, 1965.
(A.10) S.C. Batterman, Israel J. Technology, 9, No.5, 1971.
(A.11) J.W. Hutchinson, Conference on Computer-Oriented Analysis of Shell Structures, Palo Alto, California, 1970.

SUMMARY

The influence of random imperfections and inelastic deformations on the buckling and post-buckling behaviour of structures has been examined in several cases.

The financial support of the Italian National Research Council (CNR) is acknowledged.

Leere Seite
Blank page
Page vide